How to cite: *Angew. Chem. Int. Ed.* **2020**, *59*, 19618–19622
International Edition: doi.org/10.1002/anie.202006596
German Edition: doi.org/10.1002/ange.202006596

VIP Metal Recovery Very Important Paper

A Porous Organic Polymer Nanotrap for Efficient Extraction of Palladium

Briana Aguila, Qi Sun, Harper C. Cassady, Chuan Shan, Zhiqiang Liang, Abdullah M. Al-Enizic, Ayman Nafadyc, Joshua T. Wright, Robert W. Meulenberg, and Shengqian Ma**

Abstract: *To offset the environmental impact of platinum-group element (PGE) mining, recycling techniques are being explored. Porous organic polymers (POPs) have shown significant promise owing to their selectivity and ability to withstand harsh conditions. A series of pyridine-based POP nanotraps, POP-Py, POP-pNH_2-Py, and POP-oNH_2-Py, have been designed and systematically explored for the capture of palladium, one of the most utilized PGEs. All of the POP nanotraps demonstrated record uptakes and rapid capture, with the amino group shown to be vital in improving performance. Further testing on the POP nanotrap regeneration and selectivity found that POP-oNH_2-Py outperformed POP-pNH_2-Py. Single-crystal X-ray analysis indicated that POP-oNH_2-Py provided a stronger complex compared to POP-pNH_2-Py owing to the intramolecular hydrogen bonding between the amino group and coordinated chlorine molecules. These results demonstrate how slight modifications to adsorbents can maximize their performance.*

Platinum-group elements (PGEs) are recognized for their unique properties such as corrosion resistance, high melting point, and catalytic qualities. These features have made them economically invaluable, with widespread use in a variety of industrial sectors. Elements in this category, namely platinum, palladium, rhodium, ruthenium, iridium, and osmium, are employed in catalytic processes, and are vital to the electronic and automotive industries.[1] However, the ubiquitous nature of their application has put a strain on the already rare terrestrial ores. Currently, 90% of the PGE supply comes from South Africa and Russia, with the rest of the world heavily reliant on imports.[2] With increasing demands, a secondary source of these precious metals is required to keep up with consumer needs.

Recovery of PGEs from spent processes is a promising alternative to reduce the dependence on an already finite supply. Stripping electronic waste of precious metals for recycling has already been explored to some effectiveness.[3] Harsh chemical treatments are typically used however, necessitating the search for an environmentally benign option. Adsorbents, such as metal–organic frameworks,[4] silica materials,[5] and biosorbents,[6] have thus been studied to capture PGEs in the aqueous phase. This method would not only reduce the use of chemical treatments, but also open up a new avenue of resource recovery through the capture of precious metals from industrial waste streams. To do so would require an adsorbent material with exceptional selectivity and affinity for the analyte of choice, given the diverse composition of industrial processes with low concentration of PGEs.[5d,7] Current materials, however, cannot meet all the requirements of high uptake capacity, fast kinetics, exceptional selectivity/affinity, and facile recyclability despite their preliminary success, thereby urging the development of new types of adsorbents for PGE capture with superior performance.

Porous organic polymers (POPs) are a class of adsorbent material with great promise for such a challenging adsorption process. POPs are formed from purely organic building blocks connected by strong covalent bonds.[8] This produces a material with functionality and exceptional stability, a combination that most existing adsorbent materials lack. Tunable monomeric units have resulted in the use of POPs in many applications, such as catalysis,[9] gas storage,[10] and water treatment,[11] with encouraging outcomes. From this tunability, structural modifications can go even further to enhance the performance of binding sites.

Many strategies have been used to improve binding with regards to host–guest interactions. This would include pre-organization, cooperativity, and several non-covalent interactions, which have been successful for a variety of compounds.[12] Previous work in our laboratory used some of these methods to design a bio-inspired uranium coordination environment where the de novo introduction of an assistant group reinforced the interaction between the POP binding site and uranyl ions.[13] With promising results from this work,

[*] Dr. B. Aguila, H. C. Cassady, C. Shan, Prof. S. Ma
Department of Chemistry, University of South Florida
4202 E Fowler Ave., Tampa, FL 33620 (USA)
E-mail: sqma@usf.edu
Dr. Q. Sun
Key Laboratory of Biomass Chemical Engineering
College of Chemical and Biological Engineering
Zheijang University, Hangzhou, 310027 (P. R. China)
E-mail: sunqichs@zju.edu.cn
Prof. Z. Liang
State Key Lab of Inorganic Synthesis and Preparative Chemistry
Jilin University, Changchun, 130012 (P. R. China)
Prof. A. M. Al-Enizic, Prof. A. Nafadyc
Chemistry Department, King Saud University
Riyadh, 11451 (Saudi Arabia)
Dr. J. T. Wright
Department of Physics, Illinois Institute of Technology
Chicago, IL 60616 (USA)
Prof. R. W. Meulenberg
Department of Physics and Astronomy and
Frontier Institute for Research in Sensor Technologies
University of Maine, Orono, ME 04469 (USA)
Supporting information and the ORCID identification number(s) for the author(s) of this article can be found under: https://doi.org/10.1002/anie.202006596.

we took this approach to a new model system to determine if this strategy could be applied for capture and recycling of the rare platinum group elements.

In this study, we focus on the adsorption of the precious metal palladium, given its wide industrial use.[14] A series of pyridine-based POPs were rationally designed, wherein the nitrogen of the pyridine monomeric unit provides a Lewis base site to coordinate to palladium.[15] The introduction of an amino group, as well as the effects from its relative location, was further investigated. Through analysis of the maximum uptake capacity, kinetic efficiency, selectivity, and chemical stability, it was determined that the addition of the amino group increased the nucleophilicity of the pyridine binding site. Furthermore, by placing the amino group in the *ortho* position, a stronger complex with palladium could be achieved as illustrated by X-ray photoelectron spectroscopy and single-crystal X-ray data. These results guide future design strategies to enhance adsorbents for precious metal recovery under real-world conditions.

To prepare the POPs, vinyl-based monomers were first synthesized and denoted as V-Py, V-*p*NH_2-Py, and V-*o*NH_2-Py (experimental details in the Supporting Information). The monomers were cross-linked via radical polymerization to successfully transform to the final polymeric materials, coined as POP-Py, POP-*p*NH_2-Py, and POP-*o*NH_2-Py, respectively, which were subsequently investigated for their physical properties through nitrogen sorption measurements and scanning electron microscopy images (SEM). All POP materials exhibited a combination of micro- and mesopores as indicated by the nonlocal density functional theory (NLDFT) pore size distribution (Supporting Information, Figure S1) and N_2 sorption isotherms, with a steep incline at low pressure along with a hysteresis loop during the desorption process (Figure 1). From the isotherms the surface areas were calculated using the Brunauer–Emmett–Teller (BET) method. All materials had moderate to high surface area with values of 979, 536, and 359 $m^2 g^{-1}$ for POP-Py, POP-*p*NH_2-Py, and POP-*o*NH_2-Py, respectively. SEM images also show a variation in the pore size (Supporting Information, Figure S2), with the visible larger pores facilitating mass transfer and the smaller pores serving as a trap to enrich the materials for greater adsorption performance.

Following characterization, they were tested to determine their maximum capacity for palladium adsorption. To obtain adsorption isotherms, solutions of increasing Pd^{2+} concentrations (25–800 ppm) were treated with the adsorbents. After stirring overnight to achieve equilibrium, the solutions were filtered, and analyzed via ICP to determine the residual Pd^{2+} concentration. From the adsorption isotherms (Figure 2A),

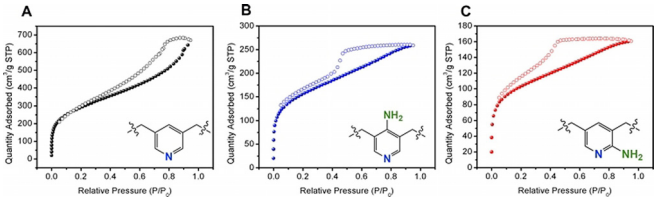

Figure 1. Nitrogen sorption isotherms of A) POP-Py, B) POP-*p*NH_2-Py, and C) POP-*o*NH_2-Py.

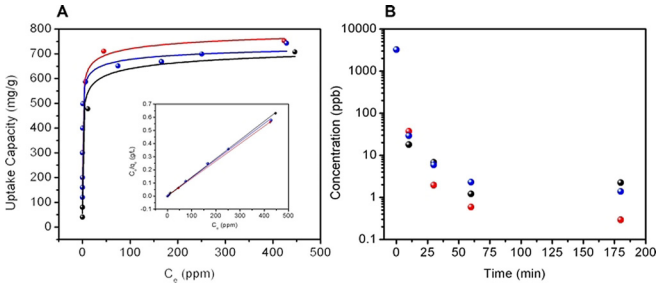

Figure 2. A) Palladium adsorption isotherms (inset: linear regression fit with the Langmuir model) and B) kinetic performance of POP-Py (black), POP-*p*NH_2-Py (blue), and POP-*o*NH_2-Py (red).

POP-Py, POP-*p*NH_2-Py, and POP-*o*NH_2-Py were fit with the Langmuir model with uptake capacities of 708, 743, and 752 mg g^{-1}, respectively. All of the materials produced record high palladium uptakes,[4,5a–c,6c,d,16] with the addition of the amino group further improving the uptake performance. Typically, a higher surface area results in enhanced adsorption performance through the availability of more exposed binding sites, however, in this work we see the opposite trend for the pyridine-based POPs. The effects of a decreased surface area for the amino-functionalized POPs is overcome by their electron donating ability, resulting in a more basic pyridine binding site and thus enhanced adsorption performance compared to POP-Py.

Given the promising results for the uptake of palladium, the adsorbent materials were studied for their kinetic efficiency. With 20 mg of the materials in 200 mL of a 5 ppm Pd^{2+} solution, 3 mL aliquots were collected at increasing time intervals. The filtrates were analyzed by ICP-MS for the remaining palladium in solution and the concentration changes were measured over time (Figure 2B). All of the adsorbents reduced the palladium concentration to ppb level within 10 minutes, and after a 3 h period the remaining concentration in solution was 2.23, 1.38, and 0.29 ppb for POP-Py, POP-*p*NH_2-Py, and POP-*o*NH_2-Py, respectively. The kinetic data were fit to a pseudo second-order kinetic model (Supporting Information, Figure S3), indicating that the rate-limiting step is a chemisorption process. Given that all of the adsorbents have a mixture of micro- and mesopores, the rapid removal is partly attributed to the hierarchical porosity, creating a nanotrap to efficiently capture palladium in solution.[17] Additionally, each monomeric unit is equipped with a pyridine group providing a large number of binding sites to complex with palladium. POP-*o*NH_2-Py shows the greatest level of efficacy of all tested adsorbents, reducing to sub-ppb level after a short treatment time. If these adsorbents are to be put into practice, not only is a high capacity beneficial but also important to have palladium capture at low concentrations.

Based on the equilibrium results from the kinetic data, the binding affinity of each adsorbent was quantified. To do so, the distribution coefficient (K_d) was calculated, with values of 1.5×10^7, 2.4×10^7, and 1.1×10^8 mL g^{-1} for POP-Py, POP-*p*NH_2-Py, and POP-*o*NH_2-Py, respectively. It is evident that POP-*o*NH_2-Py demonstrates the strongest binding by an order of magnitude, followed by POP-*p*NH_2-Py and POP-Py,

verifying the experimental capacity and kinetic data. The electron-donating capability of the additional amino group adds electron density to the π system; this in turn makes the pyridine more nucleophilic and is responsible for the enhanced performance of POP-oNH$_2$-Py and POP-pNH$_2$-Py over POP-Py. Thus, the amino functionalized POPs were the focus of further studies.

After palladium is adsorbed, it must be effectively eluted from the material to recover it for reuse, while also recycling the adsorbent. To probe this, the palladium-contacted adsorbents, Pd@POP-pNH$_2$-Py and Pd@POP-oNH$_2$-Py, were eluted using a thiourea/HCl solution. Subsequently, the regenerated adsorbents were stirred in 200 mL of a 5 ppm Pd^{2+} solution overnight. The residual concentration was measured with ICP-MS and quantified to be 29 and 0.1 ppb for POP-pNH$_2$-Py and POP-oNH$_2$-Py, respectively. The performance of POP-oNH$_2$-Py is completely maintained after recycling, while POP-pNH$_2$-Py is noticeably hindered, resulting in a residual concentration over forty times that of the pristine sample after overnight treatment (Supporting Information, Figure S4). To illustrate this phenomenon, the binding of palladium to POP-oNH$_2$-Py was investigated through X-ray photoelectron spectroscopy (XPS). The Pd 3d spectrum was collected for Pd@POP-oNH$_2$-Py to verify the adsorption process with two distinct peaks at 343.3 and 338.2 eV corresponding to $3d_{3/2}$ and $3d_{5/2}$, respectively.[18] Comparing this to the pristine and the recycled POP-oNH$_2$-Py sample, which had no discernable Pd 3d peaks, confirming the ability to elute the palladium from the adsorbent and the effectiveness of the regeneration process (Figure 3 A). The N 1s spectra further substantiates this, with the pristine sample having a N 1s peak at 399.3 eV; however, after binding with palladium this peak is shifted to 399.6 eV, indicating an interaction has occurred with the nitrogen groups of POP-oNH$_2$-Py.[19] After the material was regenerated, this peak is identical to the pristine sample with the N 1s peak at 399.3 eV (Figure 3 B). These results indicate the potential this material has for multiple adsorption cycles, extending the adsorbent lifetime in practice.

The selectivity of POP-pNH$_2$-Py and POP-oNH$_2$-Py for palladium in the presence of other ions prevalent in waste streams was then tested.[7c,20] 5 mg of adsorbent was placed in 50 mL of a 5 ppm mixed metal solution containing Pd^{2+}, Fe^{2+}, Zn^{2+}, Pb^{2+}, Ni^{2+}, and Cd^{2+}. After overnight treatment, the remaining palladium in solution was measured with ICP-MS.

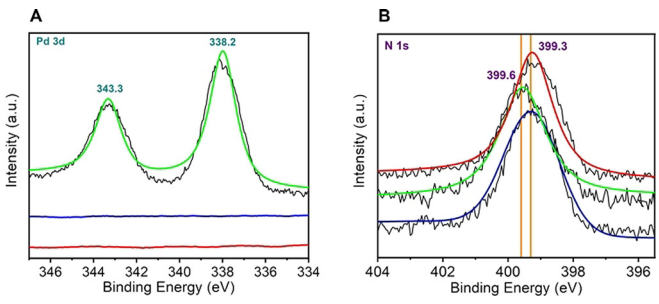

Figure 3. A) Pd 3d and B) N 1s XPS spectra of pristine (blue), palladium contacted (green), and regenerated (red) POP-oNH$_2$-Py.

POP-oNH$_2$-Py exhibited almost full palladium recovery, reducing the concentration to 1.02 ppb. Meanwhile, POP-pNH$_2$-Py showed severely reduced capacity, only decreasing the concentration to 188 ppb. Although at high concentrations the amino group in POP-pNH$_2$-Py is available as a weaker secondary binding site, it is evident that the amino group in the *ortho* position creates a more stable complex with palladium and is beneficial to selectively capture palladium at low concentrations (Figure 4).

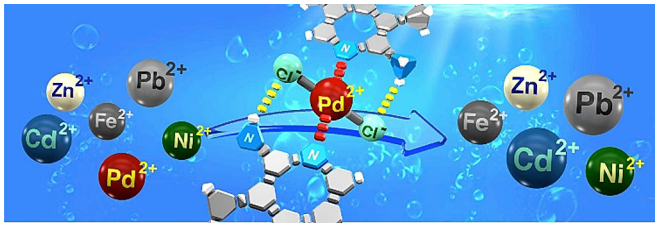

Figure 4. Illustration of Pd^{2+} selectivity over other common ions for POP-oNH$_2$-Py.

Owing to the encouraging results for POP-oNH$_2$-Py, it was used for a final analysis of the stability and performance under extreme pH conditions. 5 mg of adsorbent was placed in aqueous solutions of pH 3 and 10, respectively, and allowed to soak over a 3 day period. The adsorbents were collected and immediately used for the recovery of a 5 ppm palladium solution (50 mL) at pH 3 and 10. The residual concentration after stirring overnight was measured with ICP-MS to be 2.08 and 6.14 ppb for pH 3 and 10, respectively. The structural integrity and palladium uptake after exposure to extreme conditions demonstrates the full applicability of POP-oNH$_2$-Py for palladium recovery.

To understand the interaction between palladium and the amino-functionalized POPs, Fourier-transform infrared (FTIR) spectroscopy was conducted on the pristine and palladium-contacted samples. As seen from the Supporting Information, Figure S5, Pd@pNH$_2$-Py and Pd@oNH$_2$-Py both have an additional peak between 568–575 cm^{-1} corresponding to Pd–N stretching.[21] With the variation in intensity and the location in the fingerprint region FTIR alone is not sufficient for characterization. Further analysis was done through the collection of SEM images and energy dispersive X-ray (EDX) mapping of Pd@pNH$_2$-Py and Pd@oNH$_2$-Py (Supporting Information, Figure S6). From the images we see a homogenous distribution of palladium throughout the samples, which is in line with the monolayer adsorption process indicated by the adsorption isotherms.

Given the amorphous nature of POPs, it is challenging to determine exact structural distinctions, in particular when the same functionalities are present. Therefore, to elucidate the differences in the performance of POP-pNH$_2$-Py and POP-oNH$_2$-Py, monomeric equivalents were complexed with the palladium salt and single crystals were obtained, denoted Pd@pNH$_2$-Py and Pd@oNH$_2$-Py, respectively. As seen in Figure 5, Pd@pNH$_2$-Py was shown to have preferential binding of four pyridine units to one palladium, whereas for Pd@oNH$_2$-Py there is steric hindrance from the amino group

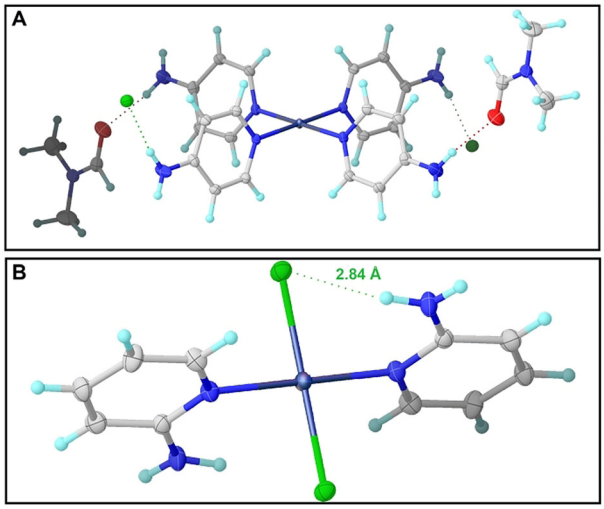

Figure 5. Single-crystal structures of A) Pd@*p*NH_2-Py (shown with coordinated DMF solvent molecules) and B) Pd@*o*NH_2-Py.[22]

in the *ortho* position reducing the coordination of pyridine to two. However, for POP-*p*NH_2-Py the amorphous polymer form would impede the ability to coordinate four pyridines to one palladium. This is further shown by the maximum uptake capacity values, wherein both polymers bind to palladium closer to a 2:1 manner. The EDX mapping images substantiate this showing the presence of Cl in both samples (Supporting Information, Figure S6), indicating palladium is coordinated to two N and two Cl groups in Pd@*p*NH_2-Py and Pd@*o*NH_2-Py. Additionally, through a combined analysis of X-ray absorption near edge structure and extended X-ray absorption fine structure studies (Supporting Information, Figures S7–S9) it was concluded that the Pd is bound to N atoms with similar bond lengths and coordination fashion for both POP-*p*NH_2-Py and POP-*o*NH_2-Py (Supporting Information, Table S3). Returning to the single-crystal data, the difference in performance can be attributed to the intramolecular hydrogen bonding between the Cl groups from the palladium salt and the amino group in the *ortho* position of Pd@*o*NH_2-Py (Figure 5 B). This in turn stabilizes the complex and allows for POP-*o*NH_2-Py to selectively capture palladium at more environmentally relevant concentrations compared to POP-*p*NH_2-Py.

In summary, through a comparative study of a series of pyridine-based POPs, POP-Py, POP-*p*NH_2-Py, and POP-*o*NH_2-Py, their ability to recover palladium was investigated. All of the adsorbents had record high uptakes with the ability to reduce the palladium concentration to ppb level. The addition of the amino group in POP-*p*NH_2-Py and POP-*o*NH_2-Py was shown to enhance the palladium recovery performance by increasing the nucleophilicity of the pyridine binding site. Additionally, the amino group in the *ortho* position relative to the pyridine binding site provided a stronger complex with palladium compared to its *para* counterpart due to the hydrogen bonding interaction between the amino group and coordinated chloride ligand as confirmed by single-crystal data. This resulted in POP-*o*NH_2-Py outperforming POP-*p*NH_2-Py with regard to regenerative abilities and selectivity, with additional successful palladium uptake experiments after exposure to extreme pH conditions. A strong binding affinity for POP-*o*NH_2-Py was calculated based on experimental equilibrium data, which was corroborated by XPS analysis of Pd 3d and N 1s. These results demonstrate how slight modifications to adsorbents can maximize their performance, which could be extended to a multitude of applications.

Acknowledgements

The authors acknowledge the U.S. National Science Foundation (CBET-1706025) for financial support of this work. Partial support from the Distinguished Scientist Fellowship Program (DSFP) at King Saud University (S.M./A.M.A.), the 111 Project (Grant No. B17020) from National Natural Science Foundation of China (Z.L.), and the U.S. National Science Foundation, DMR-1708617 (R.W.M./J.T.W.) is also acknowledged.

Conflict of interest

The authors declare no conflict of interest.

Keywords: enhanced binding affinity · hydrogen bond stabilization · palladium recovery · platinum group elements · porous organic polymers

[1] a) S. Zhang, Y. Ding, B. Liu, C.-c. Chang, *Waste Manage.* **2017**, *65*, 113–127; b) M. L. Zientek, P. J. Loferski, Platinum-Group Elements-So Many Excellent Properties: U.S. Geological Survey Fact Sheet 2014, **2014**; c) V. Fernandez, *Int. Rev. Financ. Anal.* **2017**, *52*, 333–347; d) T. Bossi, J. Gediga, *Johnson Matthey Technol. Rev.* **2017**, *61*, 111–121.

[2] a) G. M. Mudd, *Ore Geol. Rev.* **2012**, *46*, 106–117; b) J. E. Mungall, A. J. Naldrett, *Elements* **2008**, *4*, 253–258; c) D. R. Wilburn, D. I. Bleiwas, *Platinum-Group Metals- World Supply and Demand*, US Geological Survey Open-File Report 2004-1224, US Department of the Interior, Washington, DC, **2005**.

[3] a) E. Hsu, K. Barmak, A. C. West, A.-H. A. Park, *Green Chem.* **2019**, *21*, 919–936; b) B. H. Robinson, *Sci. Total Environ.* **2009**, *408*, 183–191; c) P. Tanskanen, *Acta Mater.* **2013**, *61*, 1001–1011; d) H.-Y. Kang, J. M. Schoenung, *Resour. Conserv. Recycl.* **2005**, *45*, 368–400.

[4] a) S. Lin, D. H. K. Reddy, J. K. Bediako, M.-H. Song, W. Wei, J.-A. Kim, Y.-S. Yun, *J. Mater. Chem. A* **2017**, *5*, 13557–13564; b) M. Zha, J. Liu, Y.-L. Wong, Z. Xu, *J. Mater. Chem. A* **2015**, *3*, 3928–3934.

[5] a) T. Kang, Y. Park, K. Choi, J. S. Lee, J. Yi, *J. Mater. Chem.* **2004**, *14*, 1043–1049; b) R. K. Sharma, A. Pandey, S. Gulati, A. Adholeya, *J. Hazard. Mater.* **2012**, *209*, 285–292; c) F. Bai, G. Ye, G. Chen, J. Wei, J. Wang, J. Chen, *Sep. Purif. Technol.* **2013**, *106*, 38–46; d) J. Kramer, N. E. Dhladhla, K. R. Koch, *Sep. Purif. Technol.* **2006**, *49*, 181–185.

[6] a) X. Chen, K. F. Lam, S. F. Mak, K. L. Yeung, *J. Hazard. Mater.* **2011**, *186*, 902–910; b) A.-E. Rotaru, W. Jiang, K. Finster, T. Skrydstrup, R. L. Meyer, *Biotechnol. Bioeng.* **2012**, *109*, 1889–1897; c) S. W. Won, P. Kotte, W. Wei, A. Lim, Y.-S. Yun, *Bioresour. Technol.* **2014**, *160*, 203–212; d) J. R. Dodson, H. L.

Parker, A. M. García, A. Hicken, K. Asemave, T. J. Farmer, H. He, J. H. Clark, A. J. Hunt, *Green Chem.* **2015**, *17*, 1951 – 1965.
[7] a) J. S. Guest, S. J. Skerlos, J. L. Barnard, M. B. Beck, G. T. Daigger, H. Hilger, S. J. Jackson, K. Karvazy, L. Kelly, L. Macpherson, J. R. Mihelcic, A. Pramanik, L. Raskin, M. C. M. Van Loosdrecht, D. Yeh, N. G. Love, *Environ. Sci. Technol.* **2009**, *43*, 6126 – 6130; b) T. Kakoi, N. Horinouchi, M. Goto, F. Nakashio, *J. Membr. Sci.* **1996**, *118*, 63 – 71; c) I. Matsubara, Y. Takeda, K. Ishida, *Fresenius J. Anal. Chem.* **2000**, *366*, 213 – 217.
[8] a) Y. H. Xu, S. B. Jin, H. Xu, A. Nagai, D. L. Jiang, *Chem. Soc. Rev.* **2013**, *42*, 8012 – 8031; b) N. Chaoui, M. Trunk, R. Dawson, J. Schmidt, A. Thomas, *Chem. Soc. Rev.* **2017**, *46*, 3302 – 3321; c) A. G. Slater, A. I. Cooper, *Science* **2015**, *348*, aaa8075; d) L. X. Tan, B. Tan, *Chem. Soc. Rev.* **2017**, *46*, 3322 – 3356; e) S. Das, P. Heasman, T. Ben, S. L. Qiu, *Chem. Rev.* **2017**, *117*, 1515 – 1563; f) D. Taylor, S. J. Dalgarno, Z. Xu, F. Vilela, *Chem. Soc. Rev.* **2020**, https://doi.org/10.1039/C9CS00315K; g) Y. Tian, G. Zhu, *Chem. Rev.* **2020**, https://doi.org/10.1021/acs.chemrev.9b00687.
[9] a) Y. Zhang, S. N. Riduan, *Chem. Soc. Rev.* **2012**, *41*, 2083 – 2094; b) Q. Sun, Z. F. Dai, X. J. Meng, F. S. Xiao, *Chem. Soc. Rev.* **2015**, *44*, 6018 – 6034; c) S. Kramer, N. R. Bennedsen, S. Kegnaes, *ACS Catal.* **2018**, *8*, 6961 – 6982; d) Q. Sun, B. Aguila, G. Verma, X. Liu, Z. Dai, F. Deng, X. Meng, F.-S. Xiao, S. Ma, *Chem* **2016**, *1*, 628 – 639; e) R. Cai, X. Ye, Q. Sun, Q. He, Y. He, S. Ma, X. Shi, *ACS Catal.* **2017**, *7*, 1087 – 1092; f) L. Chen, Y. Yang, Z. Guo, D. Jiang, *Adv. Mater.* **2011**, *23*, 3149 – 3154; g) T.-X. Wang, H.-P. Liang, D. A. Anito, X. Ding, B.-H. Han, *J. Mater. Chem. A* **2020**, *8*, 7003 – 7034.
[10] a) C. D. Wood, B. Tan, A. Trewin, F. Su, M. J. Rosseinsky, D. Bradshaw, Y. Sun, L. Zhou, A. I. Cooper, *Adv. Mater.* **2008**, *20*, 1916 – 1921; b) T. Ben, H. Ren, S. Ma, D. Cao, J. Lan, X. Jing, W. Wang, J. Xu, F. Deng, J. M. Simmons, S. Qiu, G. Zhu, *Angew. Chem. Int. Ed.* **2009**, *48*, 9457 – 9460; *Angew. Chem.* **2009**, *121*, 9621 – 9624; c) L. Zou, Y. Sun, S. Che, X. Yang, X. Wang, M. Bosch, Q. Wang, H. Li, M. Smith, S. Yuan, Z. Perry, H.-C. Zhou, *Adv. Mater.* **2017**, *29*, 1700229; d) J. L. Wu, F. Xu, S. M. Li, P. W. Ma, X. C. Zhang, Q. H. Liu, R. W. Fu, D. C. Wu, *Adv. Mater.* **2019**, *31*, 1802922.
[11] a) A. Alsbaiee, B. J. Smith, L. Xiao, Y. Ling, D. E. Helbling, W. R. Dichtel, *Nature* **2016**, *529*, 190; b) B. Y. Li, Y. M. Zhang, D. X. Ma, Z. Shi, S. Q. Ma, *Nat. Commun.* **2014**, *5*, 5537; c) B. Aguila, Q. Sun, J. A. Perman, L. D. Earl, C. W. Abney, R. Elzein, R. Schlaf, S. Ma, *Adv. Mater.* **2017**, *29*, 1700665; d) W. C. Wilfong, B. W. Kail, T. L. Bank, B. H. Howard, M. L. Gray, *ACS Appl. Mater. Interfaces* **2017**, *9*, 18283 – 18294; e) B. N. Zheng, X. D. Lin, X. C. Zhang, D. C. Wu, K. Matyjaszewski, *Adv. Funct. Mater.* **2019**, 1907006; f) Q. Sun, L. Zhu, B. Aguila, P. K. Thallapally, C. Xu, J. Chen, S. Wang, D. Rogers, S. Ma, *Nat. Commun.* **2019**, *10*, 1646; g) Q. Sun, B. Aguila, S. Ma, *Trends Chem.* **2019**, *1*, 292 – 303.
[12] a) R. W. Gunasekara, Y. Zhao, *Chem. Commun.* **2016**, *52*, 4345 – 4348; b) H. J. Schneider, *Angew. Chem. Int. Ed.* **2009**, *48*, 3924 – 3977; *Angew. Chem.* **2009**, *121*, 3982 – 4036; c) Z. Zhong, X. Li, Y. Zhao, *J. Am. Chem. Soc.* **2011**, *133*, 8862 – 8865; d) A. S. Ivanov, B. F. Parker, Z. Zhang, B. Aguila, Q. Sun, S. Ma, S. Jansone-Popova, J. Arnold, R. T. Mayes, S. Dai, V. S. Bryantsev, L. Rao, I. Popovs, *Nat. Commun.* **2019**, *10*, 819; e) B. Aguila, Q. Sun, H. Cassady, C. Abney, B. Li, S. Ma, *ACS Appl. Mater. Interfaces* **2019**, *11*, 30919 – 30926; f) Q. Sun, B. Aguila, Y. Song, S. Ma, *Acc. Chem. Res.* **2020**, *53*, 812 – 821.
[13] Q. Sun, B. Aguila, J. Perman, A. S. Ivanov, V. S. Bryantsev, L. Earl, C. Abney, L. Wojtas, S. Ma, *Nat. Commun.* **2018**, *9*, 1644.
[14] a) H. Doucet, J.-C. Hierso, *Curr. Opin. Drug Discovery Dev.* **2007**, *10*, 672 – 690; b) G. Ferrier, A. Berzins, N. Davey, *Platinum Met. Rev.* **1985**, *29*, 175 – 179; c) M. Beller, T. H. Riermeier, S. Haber, H.-J. Kleiner, W. A. Herrmann, *Chem. Ber.* **1996**, *129*, 1259 – 1264; d) M. Takht Ravanchi, T. Kaghazchi, A. Kargari, *Desalination* **2009**, *235*, 199 – 244.
[15] a) G. N. Lewis, *Valence and the Structure of Atoms and Molecules*, Chemical Catalog Company, Incorporated, **1923**; b) R. G. Pearson, *J. Am. Chem. Soc.* **1963**, *85*, 3533 – 3539.
[16] a) E. Birinci, M. Gülfen, A. O. Aydın, *Hydrometallurgy* **2009**, *95*, 15 – 21; b) V. V. Kumar, C. R. Kumar, A. Suresh, S. Jayalakshmi, U. K. Mudali, N. Sivaraman, *R. Soc. Open Sci.* **2018**, *5*, 171701.
[17] a) Y. S. Ho, G. McKay, *Process Biochem.* **1999**, *34*, 451 – 465; b) Y.-S. Ho, *J. Hazard. Mater.* **2006**, *136*, 681 – 689.
[18] a) A. Drelinkiewicz, M. Hasik, M. Choczyński, *Mater. Res. Bull.* **1998**, *33*, 739 – 762; b) M. Hasik, A. Bernasik, A. Drelinkiewicz, K. Kowalski, E. Wenda, J. Camra, *Surf. Sci.* **2002**, *507*, 916 – 921; c) J. F. Moulder, J. Chastain, *Handbook of X-ray Photoelectron Spectroscopy: A Reference Book of Standard Spectra for Identification and Interpretation of XPS Data*, Physical Electronics, **1995**.
[19] E. T. Kang, K. G. Neoh, K. L. Tan, *Mol. Phys.* **1990**, *70*, 1057 – 1064.
[20] E. Lahtinen, M. M. Hanninen, K. Kinnunen, H. M. Tuononen, A. Vaisanen, K. Rissanen, M. Haukka, *Adv. Sustainable Syst.* **2018**, *2*, 1800048.
[21] J. R. Durig, R. Layton, D. W. Sink, B. R. Mitchell, *Spectrochim. Acta* **1965**, *21*, 1367 – 1378.
[22] CCDC 1995168 and 1995167 (Pd@*p*NH_2-Py and Pd@*o*NH_2-Py) contain the supplementary crystallographic data for this paper. These data are provided free of charge by The Cambridge Crystallographic Data Centre.

Manuscript received: May 6, 2020
Accepted manuscript online: May 15, 2020
Version of record online: June 9, 2020

